Internal Medicine
The Japanese Society of Internal Medicine
doi: 10.2169/internalmedicine.9565-22
Intern Med 61: 3675-3682, 2022
http://internmed.jp

【 CASE REPORT 】

Neutrophil Infiltration and Acinar-ductal Metaplasia Are the Main Pathological Findings in Pembrolizumab-induced Pancreatitis

Morihisa Hirota[1], Keigo Murakami[2], Akinobu Koiwai[1], Keita Kawamura[1], Yuki Yoshino[1], Atsuko Takasu[1], Ryo Kin[1], Tomofumi Katayama[1], Katsuya Endo[1], Takayuki Kogure[1], Takayoshi Meguro[1], Toshiharu Tabata[3], Kazuhiro Murakami[2] and Kennichi Satoh[1]

Abstract:
The histopathological findings of immune checkpoint inhibitor (ICI)-induced pancreatitis have rarely been reported. A 56-year-old man with squamous cell carcinoma of the lung with bone metastasis was being treated with pembrolizumab, an anti-programmed cell death protein-1 antibody. After 13 doses, he was referred to our department due to pancreatitis. Despite characteristic symptoms of acute pancreatitis, imaging findings were similar to those of autoimmune pancreatitis. However, a histological examination showed neutrophil-based inflammatory cell infiltration and acinar-ductal metaplasia. Immunostaining showed CD8-positive T lymphocyte infiltration. This case revealed the characteristic histopathology of pembrolizumab-induced pancreatitis, which was previously poorly understood.

Key words: immune checkpoint inhibitor, pancreatitis, pembrolizumab, endoscopic ultrasonography, adverse drug event, immunohistochemistry

(Intern Med 61: 3675-3682, 2022)
(DOI: 10.2169/internalmedicine.9565-22)

Introduction

Cancers employ numerous mechanisms to suppress the antitumor immune response, such as by upregulating coinhibitory receptors, known as immune checkpoints (1). There are currently three established cancer immunotherapies consisting of monoclonal antibodies that target immune checkpoints: cytotoxic lymphocyte-associated protein 4 (CTLA-4) and programmed cell death protein 1 (PD-1), which are receptors expressed on T lymphocytes, and ligand for PD-1 (PD-L1), which is expressed on many types of cancers.

Immune checkpoint inhibitors (ICIs) are effective but can induce immune-related adverse events (irAEs) that are autoimmune in nature. The basis for most of these adverse events is a hyperactivated T-cell response directed against normal tissue (2). ICI-induced pancreatic injury, such as symptomatic pancreatitis, asymptomatic lipase elevation, pancreatic exocrine insufficiency, and diabetes, has been described (3-5). The incidence of pancreatitis induced by PD-1 inhibitors was estimated to be as low as 0.94% in a meta-analysis of clinical trials (6). However, while there have been many case reports of ICI-induced pancreatic injury, there are only a few reports describing pathological findings. The pathological findings of ICI-induced pancreatitis described thus far include neutrophil-based infiltration and T lymphocyte-based infiltration, but these findings are inconsistent and poorly understood (7, 8).

We encountered a patient with symptomatic pembrolizumab-induced pancreatitis. The novel pathological findings from samples collected via an endoscopic ultrasound-guided fine-needle biopsy (EUS-FNB) may explain the discrepancies among previous reports.

[1]Division of Gastroenterology, Tohoku Medical and Pharmaceutical University, Japan, [2]Division of Pathology, Tohoku Medical and Pharmaceutical University, Japan and [3]Division of Chest Surgery, Tohoku Medical and Pharmaceutical University, Japan
Received: February 10, 2022; Accepted: March 22, 2022; Advance Publication by J-STAGE: May 7, 2022
Correspondence to Dr. Morihisa Hirota, morihirota7373@gmail.com

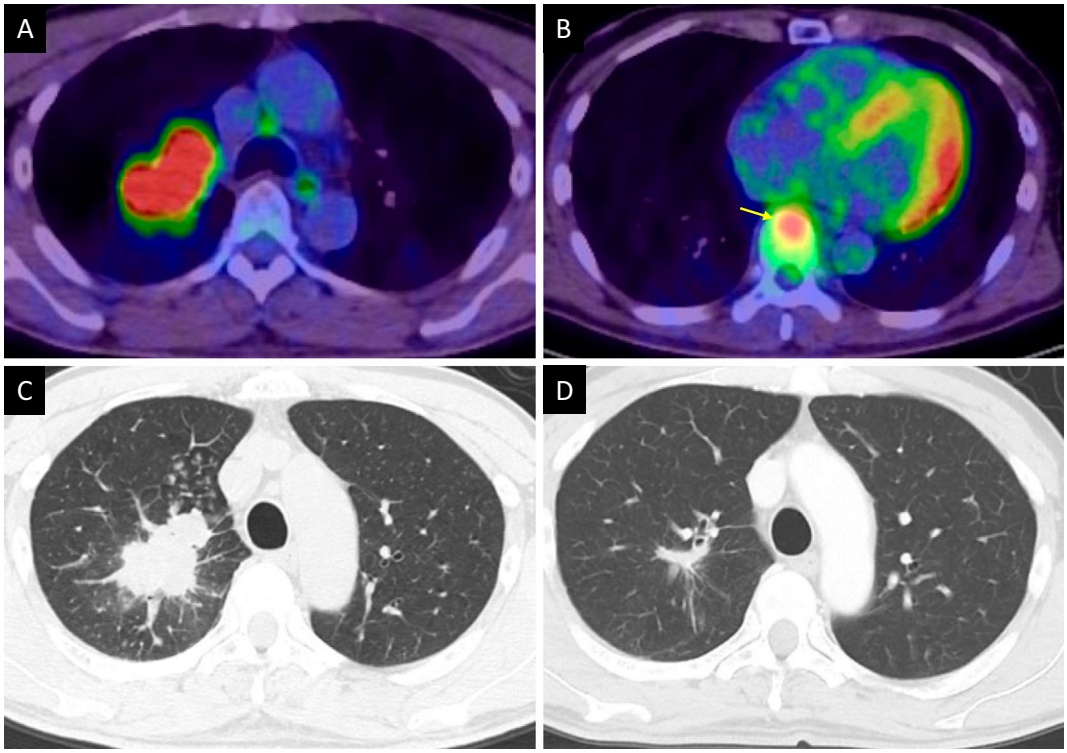

Figure 1. Imaging findings of lung cancer. FDG-PET CT showed a tumor with high uptake in the right upper lung (maximum SUV, 13.2) (A) and the T8 vertebra, which indicated bone metastasis (yellow arrow) (B). Axial CT showed an irregular tumor in the right upper lung (C). Eleven months after starting pembrolizumab, CT showed that the primary lung cancer lesion had decreased in size (D). FDG: ^{18}F-fluorodeoxyglucose, PET: positron emission tomography, CT: computed tomography, SUV: standardized uptake value

Case Report

A 56-year-old man was referred to our department due to upper abdominal pain and appetite loss for 6 days. He had no drinking history but had smoked 20 cigarettes per day for 35 years until 55 years old. He had been diagnosed with squamous cell carcinoma of the right lung with bone metastasis 10 months prior (Fig. 1A-C). Histologically, 50% of the tumor cells expressed PD-L1.

After the diagnosis, carboplatin plus nab-paclitaxel plus pembrolizumab was administered four times, which partially reduced the size of the primary lung cancer lesion (Fig. 1D). Subsequently, pembrolizumab alone was additionally administered nine times as maintenance therapy. He began to have diarrhea five to six times each day starting seven months after the initiation of pembrolizumab. Five days after the 13th administration of pembrolizumab, he suddenly developed epigastric pain and appetite loss.

He was referred to our department six days after the onset of his abdominal symptoms. At that time, his abdominal pain was alleviated but tenderness was found throughout the abdomen. No muscle guarding was found. Laboratory data were as follows: serum amylase, 500 U/L; lipase, 1,831 U/L; and C-reactive protein (CRP), 3.93 mg/dL. Contrast-enhanced computed tomography (CECT) showed diffuse enlargement of the pancreas with peripancreatic fat stranding (Fig. 2A, B). However, there was no acute peripancreatic fluid collection, which is a typical imaging finding of acute pancreatitis (AP), nor was there a capsule-like rim around the pancreas, which is a typical imaging finding of type 1 autoimmune pancreatitis (AIP), an immunoglobulin G4 (IgG 4)-related disease.

We recommended hospitalization, but he declined and went home. Three days later, he returned to our department due to persistent symptoms and was admitted. Laboratory data on admission were as follows: serum amylase, 556 U/L; lipase, 2,273 U/L; CRP, 1.89 mg/dL; IgG4, 54.0 mg/dL; and carbohydrate antigen 19-9 (CA19-9), 127.0 U/mL. These data showed sustained high levels of serum pancreatic enzymes, mildly decreased inflammation, normal serum IgG4 levels, and abnormally high levels of the tumor marker CA19-9. After admission, an elemental diet was continued for six days and then changed to a low-fat diet (9). Because he was not dehydrated, early aggressive fluid hydration was not performed.

Magnetic resonance cholangiopancreatography (MRCP) showed irregular narrowing of the main pancreatic duct in the head and tail and localized stricture of the distal common bile duct, even though laboratory data did not show liver dysfunction (Fig. 2C). Endoscopic ultrasonography (EUS) showed a diffusely enlarged and extremely hy-

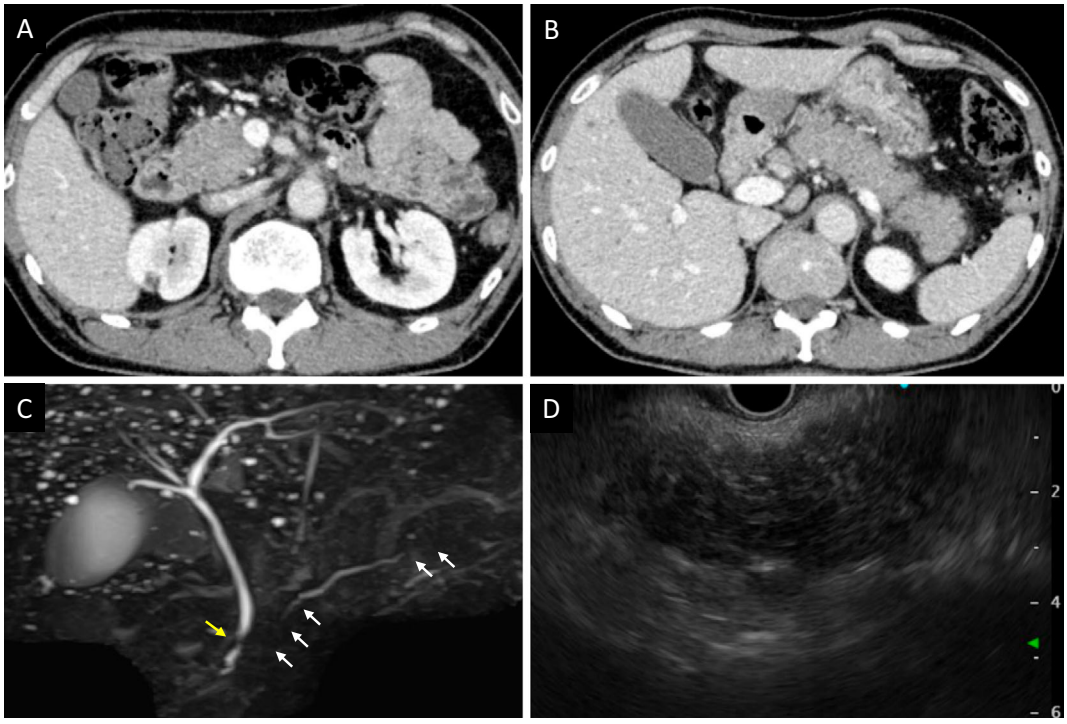

Figure 2. **Imaging findings of the pancreas. CECT showed diffuse enlargement of the pancreas, peripancreatic fat stranding, no acute peripancreatic fluid collection, and no capsule-like rim in the head of the pancreas (A) or from the body of the pancreas to the tail (B). MRCP showed irregular narrowing of the main pancreatic duct in the head and tail (white arrows) and localized stricture of the distal common bile duct (yellow arrow) (C). On EUS, a diffusely hypoechoic and enlarged pancreas was observed (D). CECT: contrast-enhanced computed tomography, MRCP: magnetic resonance cholangiopancreatography, EUS: endoscopic ultrasonography**

poechoic pancreas, similar to findings in both type 1 and type 2 AIP (Fig. 2D). These data indicated that his illness was not typical AP. We could not rule out the possibility of a diffuse atypical malignant tumor, although no obvious mass was detected in the pancreas. We performed an EUS-FNB that targeted the head of the pancreas using a 22-gauge Aquire needle (Boston Scientific, Marlborough, USA) because the distal common bile duct and main pancreatic duct in the region had narrowed. We were able to obtain enough tissue with a single puncture. Since sufficient specimens were reportedly able to be obtained for immunostaining with a 22-gauge needle, we used a 22-gauge needle instead of a 19-gauge needle for the EUS-FNB (10).

Staining of the tissue sample with Hematoxylin and Eosin (HE) showed that massive neutrophil infiltration and acinar-ductal metaplasia were the primary histological findings, with some fibrosis observed as well (Fig. 3A). No malignant cells were observed. The histological findings were not typical of AP because fat necrosis in the pancreas was not observed (Fig. 3B). Immunohistochemical staining showed no IgG4-positive plasma cells (Fig. 4A, B). Neither storiform fibrosis nor obliterative phlebitis, which are typical histological findings of type 1 AIP, was found by elastica-Masson staining (Fig. 4C, D). Many CD3-positive T lymphocytes had infiltrated the pancreas along with a few CD20-positive B lymphocytes (Fig. 5A-C). There were many CD8-positive T lymphocytes in the pancreas; some of them had directly infiltrated the acinar-ductal metaplasia (Fig. 5D). Colonoscopy showed edematous mucosa with mild redness. An HE-stained biopsy sample showed marked lymphocyte infiltration and apoptosis of the crypt cells (Fig. 6A). Immunohistochemical examinations of the colon biopsy sample showed low infiltration of CD20-positive B lymphocytes but high infiltration of CD3-positive T lymphocytes (Fig. 6B, C). Most infiltrations contained CD8-positive T lymphocytes, and some had directly infiltrated the crypts (Fig. 6D).

Given the above findings, we diagnosed the patient with pembrolizumab-induced pancreatitis and colitis, including Grade 3 pancreatitis, Grade 4 lipase elevation, and Grade 1 colitis according to the Common Terminology Criteria for Adverse Events, version 5.0. Therefore, in addition to discontinuing pembrolizumab, oral steroid administration was started at 1 mg/kg/day (3, 11).

His symptoms improved with decrease in the serum amylase and lipase levels (Fig. 7A). CECT performed four weeks after the start of steroid therapy showed marked reductions in pancreatic enlargement and peripancreatic fat stranding (Fig. 7B, C). Serum CA19-9 decreased to the normal range (36.3 U/mL) at 6 months after the start of steroid therapy.

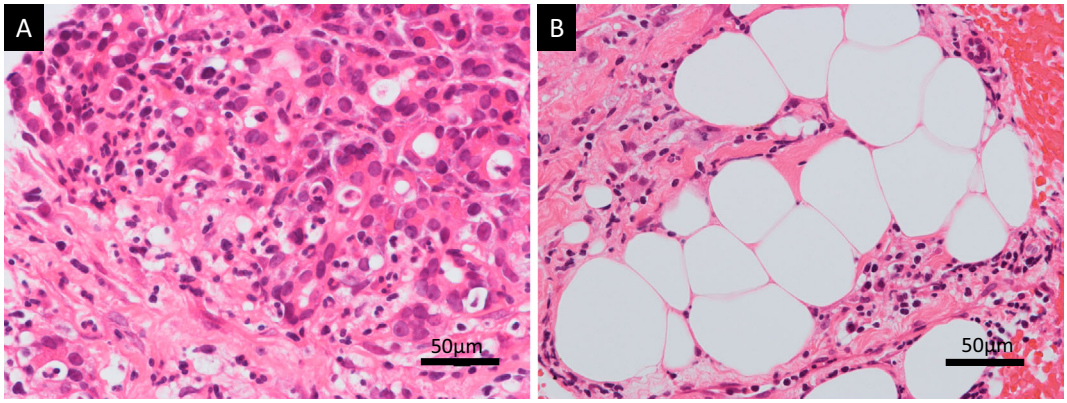

Figure 3. **Lack of typical histological findings for AP. Hematoxylin and Eosin staining of the EUS-FNB sample in high magnification showed that neutrophil infiltration and acinar-ductal metaplasia were the primary histological findings (A). Fat deposition was found in the pancreas, but there was no fat necrosis detected, which is a typical finding of AP (B). AP: acute pancreatitis, EUS: endoscopic ultrasonography, FNB: fine-needle biopsy**

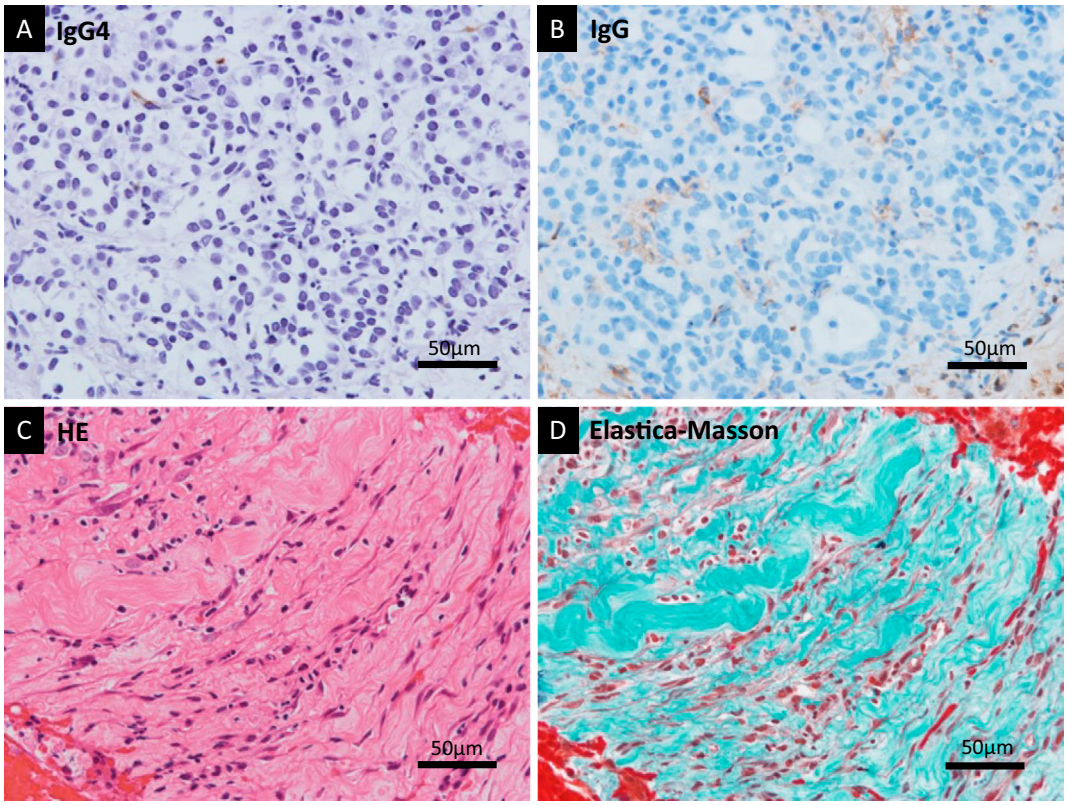

Figure 4. **Lack of typical histological findings for AIP. Immunohistochemical staining of the EUS-FNB sample in high magnification showed no IgG4-positive plasma cells (A). IgG staining was a control to show background staining (B). Storiform fibrosis was not detected with HE staining (C). EM staining showed non-specific fibrosis, but no obliterative phlebitis was detected (D). AIP: autoimmune pancreatitis, EUS: endoscopic ultrasonography, FNB: fine-needle biopsy, IgG4: immunoglobulin G4, HE: Hematoxylin and Eosin staining, EM: elastica-Masson**

Discussion

irAEs are disorders caused by an autoimmune response to normal tissues. This phenomenon is mainly due to direct immune responses to normal tissues by hyperactivated T lymphocytes and includes toxicity due to cytokines released by CD4-positive helper T lymphocytes and direct cellular injury by CD8-positive cytolytic T lymphocytes (2). According to a meta-analysis, the overall incidence of irAEs in 12,808 patients treated with anti-PD-1/PD-L1 antibodies was 26.82% [95% confidence interval (CI) 21.73-32.61%] for any grade

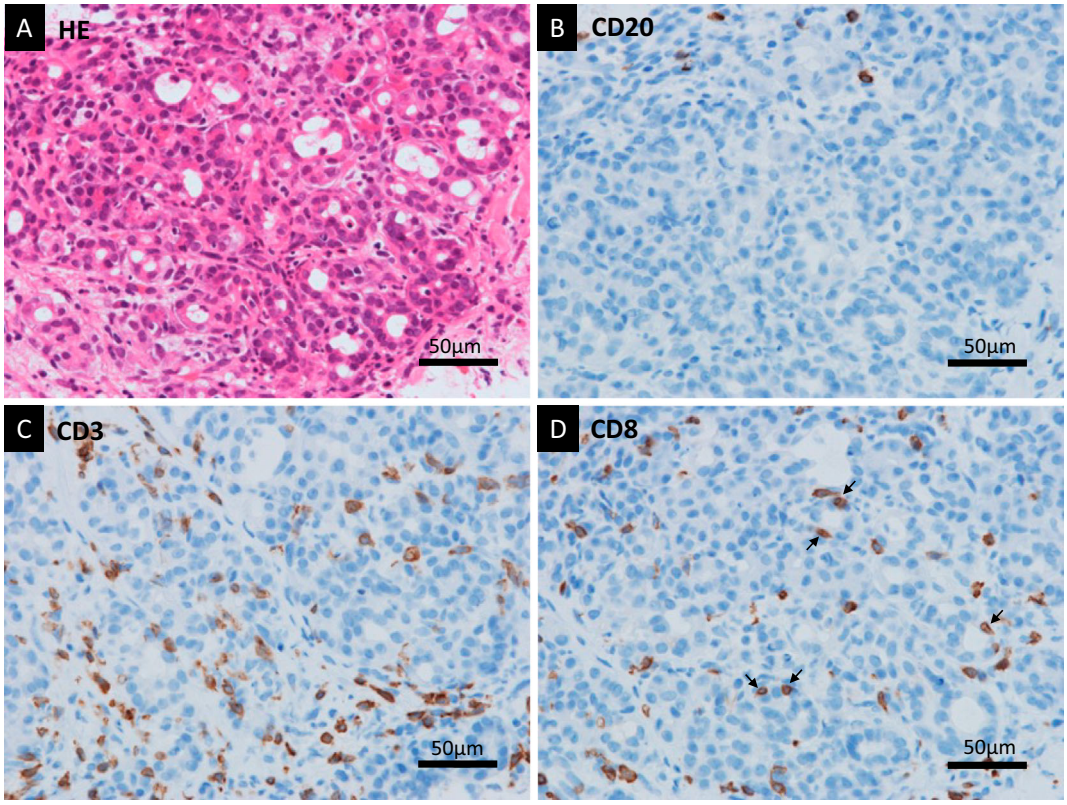

Figure 5. **T lymphocyte infiltration of the pancreas. HE staining showed neutrophil infiltration and acinar-ductal metaplasia adjacent to the immunostaining sections (A). With anti-CD20 Immunostaining, there were only a few CD20-positive B lymphocytes in a high-magnification field (B). There were abundant CD3-positive T lymphocytes detected with anti-CD3 immunostaining (C). Anti-CD8 immunostaining showed that the T lymphocytes included CD8-positive cytotoxic T lymphocytes that had infiltrated the pancreas (D). Some T lymphocytes had directly infiltrated the acinar-ductal metaplasia (arrows) (D). HE: Hematoxylin and Eosin, CD: cluster of differentiation**

and 6.10% (95% CI, 4.85-7.64%) for severe grade (12). A retrospective study of anti-PD-1 antibody treatment of 496 melanoma patients showed that 242 irAEs were observed in 138 patients (27.8%). Targeted organs by irAEs include the skin (8.7%), endocrine (6.0%), gastrointestinal system (4.3%), liver (2.2%), pancreas (1.8%), and kidney (0.4%) (3). A meta-analysis of clinical trials using ICIs showed that the incidence of asymptomatic lipase elevation was 2.7%, and that of Grade ≥2 pancreatitis was 1.9%. The incidence of pancreatitis caused by anti-PD-1 antibody (0.94%) was significantly lower than that caused by anti-CTLA-4 antibody (3.98%) (6). Recently, a fatal case of pancreatitis caused by the anti-PD-1 antibody pembrolizumab was reported for the first time (13).

Detailed histological findings of irAE-induced pancreatitis have been previously reported in two cases. However, the results were inconsistent and not well understood. Rawson et al. described a 43-year-old man who had been treated with pembrolizumab for metastatic malignant melanoma and underwent pancreaticoduodenectomy due to recurrent bowel obstruction in the annular portion of the pancreas after pembrolizumab therapy. HE-stained sections from resected tissue samples showed acute on chronic pancreatitis with marked loss of pancreatic acinar cells, replacement fibrosis, mixed acute and chronic inflammatory cell infiltrates in the interstitial tissue, and no increase in the number of IgG4-positive cells (7). They also reported typical histological findings of neutrophil aggregation in many pancreatic ducts. They did not mention pancreatic duct destruction by neutrophilic infiltration, which is a typical histological finding of type 2 AIP called a granulocytic epithelial lesion (GEL) (14). They also did not mention any immunohistopathological results (7). In contrast, Suda et al. described a 57-year-old man with simultaneous occurrence of AIP and sclerosing cholangitis-like features after pembrolizumab administration. The patient was treated with pembrolizumab for postoperative recurrence of lung cancer. He subsequently developed liver damage and AP. A liver biopsy and EUS-FNB of the pancreas were performed. The liver biopsy showed small-duct cholangitis and mild panlobular hepatitis. The infiltrating cells were mainly lymphocytes, which included CD8- and CD4-positive T lymphocytes. Tissue samples of the pancreas from EUS-FNB showed lymphocyte predominance and mild inflammatory infiltration. Immunostaining revealed more CD8-positive cell infiltrates than CD4-positive cell infiltrates (8). They did not mention or show the neutrophil aggregations in the pancreatic ducts indicated by Rawson et al. or the neutrophil-predominant infiltration and acinar-ductal meta-

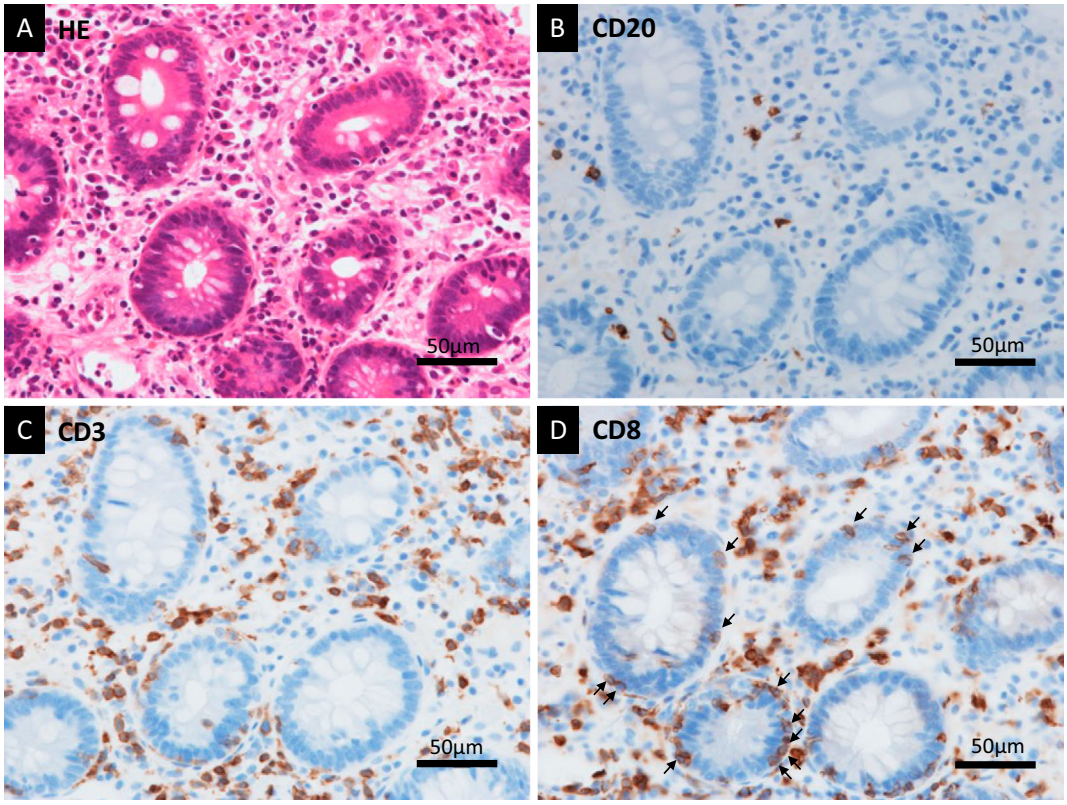

Figure 6. **Histological findings of biopsy samples from the colonic mucosa. HE staining showed marked lymphocyte infiltration and apoptosis of crypt cells (A). With anti-CD20 immunostaining, there were a small number of CD20-positive B lymphocytes in a high-magnification field (B). In contrast, there were many CD3-positive T lymphocytes detected with anti-CD3 immunostaining (C). Anti-CD8 immunostaining showed that the T lymphocytes predominantly included CD8-positive T lymphocytes (D). Some T lymphocytes had directly infiltrated the crypts (arrows) (D). HE: Hematoxylin and Eosin, CD: cluster of differentiation**

plasia presented in the present report. Thus, there were obvious differences in the pathological findings from the pancreas between the previous two reports.

In our case, HE staining showed neutrophil-dominated inflammatory cell infiltration, acinar-ductal metaplasia, and fibrosis. These findings resembled the histological findings shown by Rawson et al., but neutrophil aggregation in the pancreatic duct was not found. The lack of neutrophil aggregations in the pancreatic duct in this study might be due to EUS-FNB samples, which are usually taken while avoiding the pancreatic duct, instead of resected samples. In addition, the acinar-ductal metaplasia with neutrophilic infiltration observed in our case is a characteristic but not specific finding in biopsy samples of type 2 AIP, which is a rare type of AIP in Japan (15, 16). Recently, another report showed predominant neutrophil infiltration in pembrolizumab-induced pancreatitis in EUS-FNB samples, but detailed histological findings were not presented (17) The report also mentioned that the patient had concomitant colitis, like our patient. Histological findings, EUS and MRCP imaging findings, and concomitant colitis of that patient and our patient might suggest a similar pathology to type 2 AIP. Type 2 AIP involves an enlarged and hypoechoic pancreas with irregular narrowing of the main pancreatic duct and typical histological findings, such as GEL and acinar-ductal metaplasia with neutrophil infiltration. Type 2 AIP is reportedly associated with inflammatory bowel disease (15, 16, 18). However, the similarities between pembrolizumab-induced pancreatitis and type 2 AIP remain a question for future research.

Immunostaining of EUS-FNB samples showed T lymphocyte infiltration in the pancreatic tissue. B lymphocytes were relatively rare, but there were abundant CD8-positive T lymphocytes, including some that had infiltrated pancreatic acinar cells. These findings were identical to those observed in the colon (Fig. 6B-D) and immunohistological findings obtained by Suda et al., suggesting that an irAE due to an ICI had occurred (2, 8). Infiltrations of both CD4- and CD8-positive T cells in the pancreas have also been reported in type 1 AIP cases (19, 20). Whether or not this phenomenon is involved in the pathogenesis of type 1 AIP and whether this phenomenon is also found in type 2 AIP are unclear at present. In our case, the results suggest there might be two different causes of the histological findings in pembrolizumab-induced pancreatitis: tissue injury caused by ICI-induced hyperactivation of T lymphocytes, and excessive neutrophil infiltration, which might be related to the mechanism underlying type 2 AIP development.

A particular limitation associated with the present study is

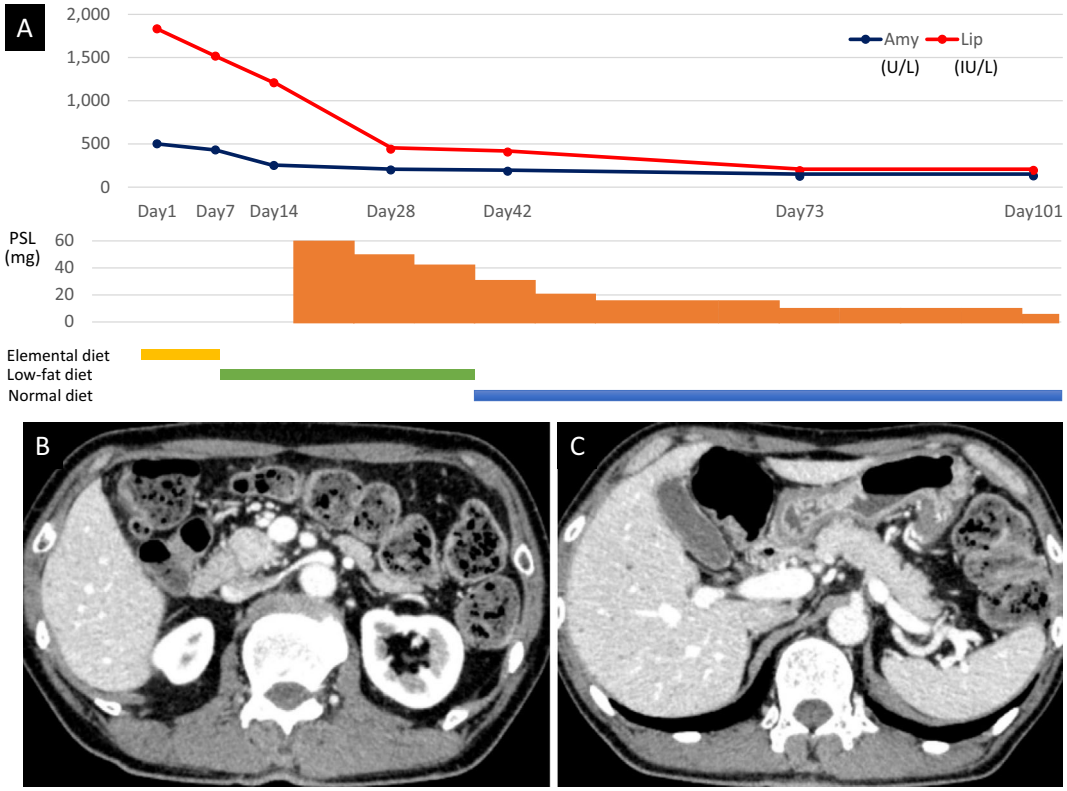

Figure 7. Improvement with steroid treatment. A diagram showing the course of steroid administration, nutrition, and pancreatic enzyme, serum amylase, and serum lipase levels (A). CECT on day 42 showed less-diffuse pancreatic enlargement and peripancreatic fat stranding in the head of the pancreas (B) and from the body to the tail of the pancreas (C). Amy: amylase, Lip: lipase, PSL: prednisolone, CECT: contrast-enhanced computed tomography

that our data are based on EUS-FNB samples. Although the report by Rawson et al. presented histological findings from resected pancreatic tissue, pancreatic resection is hardly performed for ICI-induced pancreatitis. The limitation of an EUS-FNB is that only small samples are available, because it is a needle-based biopsy. Since the puncture route avoids puncturing the pancreatic duct and blood vessels, samples obtained do not contain those types of tissue. Therefore, the reason that we did not observe neutrophil aggregation in the pancreatic duct as reported by Rawson et al. was likely because the samples obtained by the EUS-FNB did not include the pancreatic duct.

In conclusion, we described diverse histological findings in the pancreas for pembrolizumab-induced pancreatitis, which has been poorly understood. Our findings may partially explain the discrepancies in histological findings between two previously presented cases. Further research is needed to elucidate the histology and pathogenesis of ICI-induced pancreatitis.

The authors state that they have no Conflict of Interest (COI).

References

1. La-Beck NM, Jean GW, Huynh C, Alzghari SK, Lowe DB. Immune checkpoint inhibitors: new insight and current place in cancer therapy. Pharmacotherapy **35**: 963-976, 2015.
2. Weber JS, Yang JC, Atkins MB, Disis ML. Toxicities of immunotherapy for the practitioner. J Clin Oncol **33**: 2092-2099, 2015.
3. Hofmann L, Forschner A, Loquai C, et al. Cutaneous, gastrointestinal, hepatic, endocrine, and renal side-effect of anti-PD-1 therapy. Eur J Cancer **60**: 190-209, 2016.
4. Abu-Sbeih H, Tang T, Lu Y, et al. Clinical characteristics and outcomes of immune checkpoint inhibitor-induced pancreatic injury. J Immunother Cancer **7**: 31, 2019.
5. Hsu C, Marshall JL, He AR. Workup and management of immune-mediated hepatobiliary pancreatic toxicities that develop during immune checkpoint inhibitor treatment. Oncologist **25**: 105-111, 2020.
6. George J, Bajaj D, Sankaramangalam K, et al. Incidence of pancreatitis with the use of immune checkpoint inhibitors (ICI) in advanced cancers: a systematic review and meta-analysis. Pancreatology **19**: 587-594, 2019.
7. Rawson RV, Robbins E, Kapoor R, Scolyer RA, Long GV. Recurrent bowel obstruction: unusual presentation of pembrolizumab-induced pancreatitis in annular pancreas. Eur J Cancer **82**: 167-170, 2017.
8. Suda T, Kobayashi M, Kurokawa K, Matsushita E. Simultaneous occurrence of autoimmune pancreatitis and sclerosing cholangitis as immune-related adverse events of pembrolizumab. BMJ Case Rep **14**: e243360, 2021.
9. Kataoka K, Sakagami J, Hirota M, Masamune A, Shimosegawa T. Effect of oral ingestion of the elemental diet in patients with painful chronic pancreatitis in the real-life setting in Japan. Pancreas **43**: 451-457, 2014.
10. Kanno A, Ishida K, Hamada S, et al. Diagnosis of autoimmune

pancreatitis by EUS-FNA by using a 22-gauge needle based on the International Consensus Diagnostic Criteria. Gastrointest Endosc **76**: 594-602, 2012.

11. Trinh S, Le A, Gowani S, La-Beck NM. Management of immune-related adverse events associated with immune checkpoint inhibitor therapy: a minireview of current clinical guidelines. Asia Pac J Oncol Nurs **6**: 154-160, 2019.

12. Wang PF, Chen Y, Song SY, et al. Immune-related adverse events associated with anti-PD-1/PD-L1 treatment for malignancies: a meta-analysis. Pancreatology **19**: 587-594, 2019.

13. Ueno M, Tsuji Y, Yokoyama T, et al. Fatal immune checkpoint inhibitor-related pancreatitis. Intern Med **60**: 3905-3911, 2021.

14. Zamboni G, Luttges J, Capelli P, et al. Histopathological features of diagnostic and clinical relevance in autoimmune pancreatitis: a study on 53 resection specimens and 9 biopsy specimens. Virchows Arch **445**: 552-563, 2004.

15. Notohara K, Kamisawa T, Fukushima N, et al. Guidance for diagnosing autoimmune pancreatitis with biopsy tissues. Pathol Int **70**: 699-711, 2020.

16. Kamisawa T, Chari ST, Lerch MM, Kim MH, Gress TM, Shimosegawa T. Recent advances in autoimmune pancreatitis: type 1 and type 2. Gut **62**: 1373-1380, 2013.

17. Ofuji K, Hiramatsu K, Nosaka T, et al. Pembrolizumab-induced autoimmune side effects of colon and pancreas in a patient with lung cancer. Clin J Gastroenterol **14**: 1692-1699, 2021.

18. Shimosegawa T, Chari ST, Frulloni L, et al. International consensus diagnostic criteria for autoimmune pancreatitis: guidelines of the International Association of Pancreatology. Pancreas **40**: 352-358, 2011.

19. Li SY, Huang XY, Chen YT, Liu Y, Zhao S. Autoimmune pancreatitis characterized by predominant CD8+ T lymphocyte infiltration. World J Gastroentrol **17**: 4635-4639, 2011.

20. Pezzilli R, Pagano N. Pathophysiology of autoimmune pancreatitis. World J Gastrointest Pathophysiol **5**: 11-17, 2014.